



ISTITUTO NAZIONALE DI RICERCA METROLOGICA Repository Istituzionale

Evaluation of thermal gradients in longitudinal spin Seebeck effect measurements

Original

Evaluation of thermal gradients in longitudinal spin Seebeck effect measurements / Sola, Alessandro; Kuepferling, Michaela; Basso, Vittorio; Pasquale, Massimo; Kikkawa, T.; Uchida, K.; Saitoh, E.. - In: JOURNAL OF APPLIED PHYSICS. - ISSN 1089-7550. - 117:(2015).

[<http://scitation.aip.org/content/aip/journal/jap/117/17/10.1063/1.4916762>]

Availability:

This version is available at: 11696/29666 since: 2021-03-02T16:04:06Z

Publisher:

American Institute of Physics

Published

DOI:<http://scitation.aip.org/content/aip/journal/jap/117/17/10.1063/1.4916762>

Terms of use:

This article is made available under terms and conditions as specified in the corresponding bibliographic description in the repository

Publisher copyright

(Article begins on next page)

See discussions, stats, and author profiles for this publication at: <http://www.researchgate.net/publication/275223282>

Evaluation of thermal gradients in longitudinal spin Seebeck effect measurements

ARTICLE *in* JOURNAL OF APPLIED PHYSICS · MAY 2015

Impact Factor: 2.18 · DOI: 10.1063/1.4916762

READS

20

7 AUTHORS, INCLUDING:



[Michaela Kuepferling](#)

INRIM Istituto Nazionale di Ricerca Metrologica

52 PUBLICATIONS 210 CITATIONS

[SEE PROFILE](#)



[M. Pasquale](#)

INRIM Istituto Nazionale di Ricerca Metrologica

110 PUBLICATIONS 824 CITATIONS

[SEE PROFILE](#)



[Kazuharu Uchida](#)

Aichi Medical University

138 PUBLICATIONS 733 CITATIONS

[SEE PROFILE](#)

Evaluation of thermal gradients in longitudinal spin Seebeck effect measurements

A. Sola, M. Kuepferling, V. Basso, M. Pasquale, T. Kikkawa, K. Uchida, and E. Saitoh

Citation: *Journal of Applied Physics* **117**, 17C510 (2015); doi: 10.1063/1.4916762

View online: <http://dx.doi.org/10.1063/1.4916762>

View Table of Contents: <http://scitation.aip.org/content/aip/journal/jap/117/17?ver=pdfcov>

Published by the [AIP Publishing](#)

Articles you may be interested in

Joule heating-induced coexisted spin Seebeck effect and spin Hall magnetoresistance in the platinum/Y3Fe5O12 structure

Appl. Phys. Lett. **105**, 182403 (2014); 10.1063/1.4901101

Investigation of the magnetic properties of insulating thin films using the longitudinal spin Seebeck effect

J. Appl. Phys. **115**, 17C731 (2014); 10.1063/1.4864252

Thermal spin pumping and magnon-phonon-mediated spin-Seebeck effect

J. Appl. Phys. **111**, 103903 (2012); 10.1063/1.4716012

Spin current injection by spin Seebeck and spin pumping effects in yttrium iron garnet/Pt structures

J. Appl. Phys. **111**, 07C513 (2012); 10.1063/1.3676239

Observation of longitudinal spin-Seebeck effect in magnetic insulators

Appl. Phys. Lett. **97**, 172505 (2010); 10.1063/1.3507386

You don't still use this cell phone

or this computer

Why are you still using an AFM designed in the 80's?

It is time to upgrade your AFM

Minimum \$20,000 trade-in discount for purchases before August 31st

Asylum Research is today's technology leader in AFM

dropmyoldAFM@oxinst.com

OXFORD
INSTRUMENTS
The Business of Science®



Evaluation of thermal gradients in longitudinal spin Seebeck effect measurements

A. Sola,^{1,a)} M. Kuepferling,¹ V. Basso,¹ M. Pasquale,¹ T. Kikkawa,² K. Uchida,^{2,3} and E. Saitoh^{2,4,5,6}

¹*Istituto Nazionale di Ricerca Metrologica, Strada delle Cacce 91, 10135 Turin, Italy*

²*Institute for Materials Research, Tohoku University, Sendai 980-8577, Japan*

³*PRESTO, Japan Science and Technology Agency, Saitama 332-0012, Japan*

⁴*WPI Advanced Institute for Materials Research, Tohoku University, Sendai 980-8577, Japan*

⁵*CREST, Japan Science and Technology Agency, Tokyo 102-0076, Japan*

⁶*Advanced Science Research Center, Japan Atomic Energy Agency, Tokai 319-1195, Japan*

(Presented 7 November 2014; received 23 September 2014; accepted 23 November 2014; published online 6 April 2015)

In the framework of the longitudinal spin Seebeck effect (LSSE), we developed an experimental setup for the characterization of LSSE devices. This class of device consists in a layered structure formed by a substrate, a ferrimagnetic insulator (YIG) where the spin current is thermally generated, and a paramagnetic metal (Pt) for the detection of the spin current via the inverse spin-Hall effect. In this kind of experiments, the evaluation of a thermal gradient through the thin YIG layer is a crucial point. In this work, we perform an indirect determination of the thermal gradient through the measurement of the heat flux. We developed an experimental setup using Peltier cells that allow us to measure the heat flux through a given sample. In order to test the technique, a standard LSSE device produced at Tohoku University was measured. We find a spin Seebeck S_{SSE} coefficient of $2.8 \times 10^{-7} \text{ V K}^{-1}$. © 2015 AIP Publishing LLC.

[<http://dx.doi.org/10.1063/1.4916762>]

I. INTRODUCTION

The recently discovered spin Seebeck effect is the spin counterpart of the Seebeck effect and has a promising role in the field of spintronics as potential source of a thermally generated spin current.¹⁻³ The longitudinal spin Seebeck effect (LSSE) rises in a ferrimagnetic insulator, which in most of the experiments is a yttrium iron garnet layer ($\text{Y}_3\text{Fe}_5\text{O}_{12}$, YIG), subjected to a temperature difference between its surfaces.⁴ Because of the magnetic moment carried by non-equilibrium magnons, a spin current flows parallel to the direction of the temperature gradient, as shown in the sketch in Figure 1. The physical quantity related to the LSSE is the spin current over the temperature gradient across the YIG layer; however, it is necessary to introduce another phenomenon for the electrical detection of spin current. For this purpose, a paramagnetic metal with high spin Hall angle like platinum (Pt) is deposited on the interface of the ferrimagnetic insulator and it allows to detect the thermally generated spin current by the inverse spin Hall effect (ISHE).⁵ This phenomenon rises as the electrically undetectable spin current flows into the paramagnetic metal where conduction electrons are polarized and scattered according to their polarization direction. This leads to an electric potential V_x proportional to the spin current injection between the ferrimagnetic insulator and the paramagnetic metal.^{6,7} The electric field due to the ISHE can be expressed by $E_x = V_x/w_{Pt} = D_{ISHE}(J_S \times \sigma)$, where w_{Pt} is the distance between the electric contacts on the Pt strip, D_{ISHE} is the

ISHE coefficient for Pt, J_S is the spin current along the z direction, and σ is the spin polarization vector. The measurement of ISHE coupled with the LSSE allows to quantify the effect that rises in a YIG/Pt structure in terms of voltage over temperature difference. It is possible to define a spin Seebeck coefficient, as it has been done for the transversal spin Seebeck effect by others,⁸ by the expression

$$S_{SSE} \equiv \frac{E_x}{\nabla_z T} = \frac{V_x t_{YIG}}{w_{Pt} \Delta T_z}, \quad (1)$$

where t_{YIG} is the thickness of the ferrimagnetic layer, as schematically reported in Figure 1. This expression of spin Seebeck coefficient contains an indirect characterization of LSSE because of the spin current-voltage conversion efficiency at the YIG-Pt interface. Experimental artifacts related to the characterization of a LSSE device are discussed in detail.^{9,10} These are the possible contribution of anomalous Nernst effect (ANE) to the ISHE due to a static magnetic proximity effects¹¹ in Pt. In a spin Seebeck effect experiment, it was shown that the contribution of ANE can be considered as negligible.^{12,13} In Eq. (1), the most critical parameter to be determined is the temperature difference between the surfaces of the YIG layer. In our standard LSSE device, the YIG film is a few micrometers thick structure grown on a thicker gadolinium gallium garnet (GGG) substrate (see Figure 1).

If we assume that the room temperature thermal conductivities of the YIG and the GGG are the same and the thermal resistances between the layers of the structure are negligible, for the device under investigation whose YIG and GGG

^{a)}Electronic mail: a.sola@inrim.it

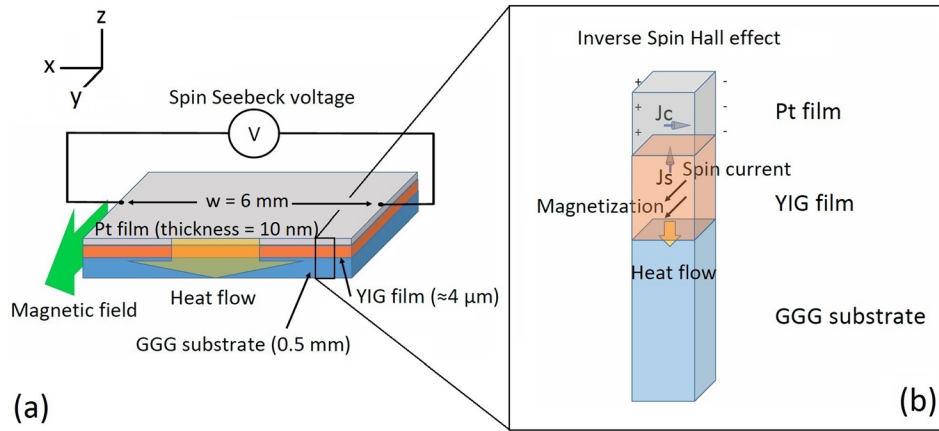


FIG. 1. Geometry of the longitudinal spin Seebeck effect: (a) schematic illustration of a LSSE device formed by a layered structure of GGG, YIG, and platinum and (b) representation of the spin current generation (LSSE) in the YIG film and detection (ISHE) in the platinum film.

thickness are $4\mu\text{m}$ and 0.5mm , respectively, a temperature difference of 1K over the sample corresponds to 8mK over the YIG layer. The value of the temperature difference across the YIG involves a non-trivial measurement because of the determination of the thermal resistance of the contacts between sample and thermometers. Only recently some efforts have been made for the improvement of the direct measurement of the temperature difference over the YIG layer,¹⁴ but this problem is little discussed in literature where usually the temperature difference across the whole sample is reported as cause of the LSSE instead of the temperature difference across the YIG film. To overcome this issue, we proposed in this work an indirect determination of ΔT_z through the measurement of the heat flux. The heat flux from a source to a heat sink through the LSSE device and a flux sensor does not depend on the thermal conductivity of the interfaces and can be easily measured by means of a calibrated heat flux sensor. In this experimental configuration, it is possible to investigate the LSSE by using the information of the thermal conductivity of YIG and its geometrical properties. This configuration allows the reproducibility of the measurement independently of thermal contacts and the comparability of results from different experimental setups.

II. EXPERIMENTAL SETUP

The measurement system, represented schematically in Figure 2, is a closed thermal circuit in which a given quantity of heat flows through elements that are in series: the thermoelectric elements used as heat flux sensors (c), the sample under investigation (f), and a couple of power Peltier cells (d), used as heat flux actuators. We use two T-type thermocouples (a) for the measurement of the temperature difference between the two brass blocks. We measure the temperature of the heat sink by a standard Pt-100 thermometer (e). The heat sink is connected to the heat flux actuators and is stabilized to room temperature by a cryo-circulator.

We calibrated the heat flux sensors by using an electric heater resistor as a known Joule heat source placed between the two heat flux sensors. The Peltier cell that we use as heat flux sensor can be described by the thermoelectric equations:¹⁵ $v = Ri + \varepsilon\Delta T$ and $q = \Pi i + \frac{1}{2}Ri^2 - K\Delta T$, in which the thermodynamic forces are the voltage v at the terminals of the Peltier cell and the temperature difference ΔT between

the two surfaces; the temperature on each surface can be considered uniform. The current involved in the working principle of the sensor are the electric current i and the heat

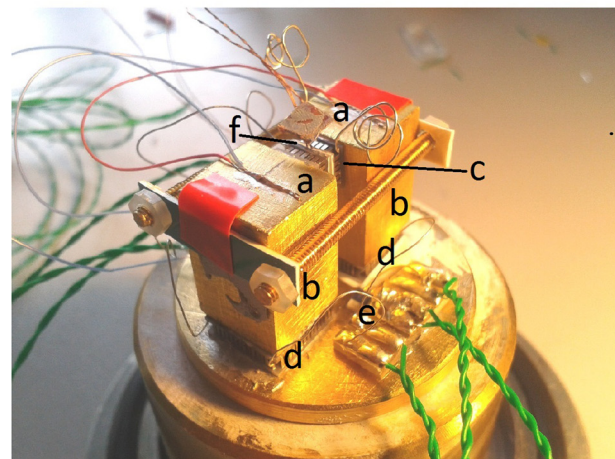
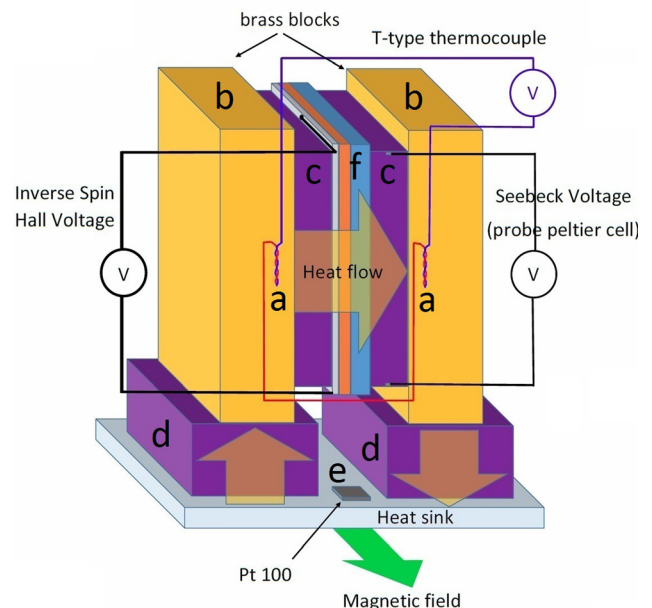


FIG. 2. Schematic illustration (top) and picture (bottom) of the experimental setup developed for the characterization of the LSSE as a function of the heat flux. (a) T-type thermocouples, (b) brass blocks, (c) Peltier cells used as heat flux sensor, (d) Pelteir cells used as heat flux actuators, (e) Pt-100 thermometer, (f) sample.

flux q . The Seebeck coefficient of the junctions is ε , Π is the Peltier coefficient, while the pillars that form the cell are described by R and K that are the total electrical resistance and thermal conductance, respectively. In open electric circuit conditions, the thermoelectric equations are reduced to $v = S_p q$, where $S_p = -\frac{\varepsilon}{K}$. The sensitivity of the heat flux sensors obtained by the calibration is $S_p = 0.934$ V/W. The spin Seebeck sample (see Figure 1) was fabricated by the Saitoh group in Tohoku University. It is a $4\ \mu\text{m}$ -thick YIG film grown on a $0.5\ \text{mm}$ -thick GGG substrate. The sample dimensions are $2\ \text{mm} \times 6\ \text{mm}$ and the thickness of the platinum film on the top of the YIG is $10\ \text{nm}$. The measurement procedure involves the production of the heat flux through the sample by means of the heat flux actuators until reaching stationary conditions. The sensor is able to monitor the heat flux through the loop, while the static external magnetic field aligns the magnetization of the YIG film. The measurement of the LSSE voltage is performed by means of a Keithley 2182A digital nanovoltmeter. The magnetic field is obtained by an electromagnet and is measured by a Hall probe gaussmeter. We performed all measurements and the calibration under vacuum (1.6×10^{-4} mbar), obtained by a turbo-molecular pump, in order to avoid conduction through air and convection.

III. RESULTS

We demonstrate the critical role played by the thermal contact in the temperature measurements and discuss the consequence on the evaluation of the thermal gradient across the YIG layer. When a sample is placed between the two heat flux sensors, we can calculate the temperature difference on the sample by the following relation: $\Delta T_{\text{sample}} = \Delta T_{\text{blocks}} - q \cdot R_{PS}$, where ΔT_{blocks} is the temperature difference measured by the thermocouples, R_{PS} is the thermal resistance of the two Peltier sensors and the thermal contact in between. R_{PS} should be carefully characterized in preliminary experiments; however, we show that R_{PS} cannot be determined with the required accuracy. The characterization is performed by putting the sensors in contact without any sample in between and by applying a

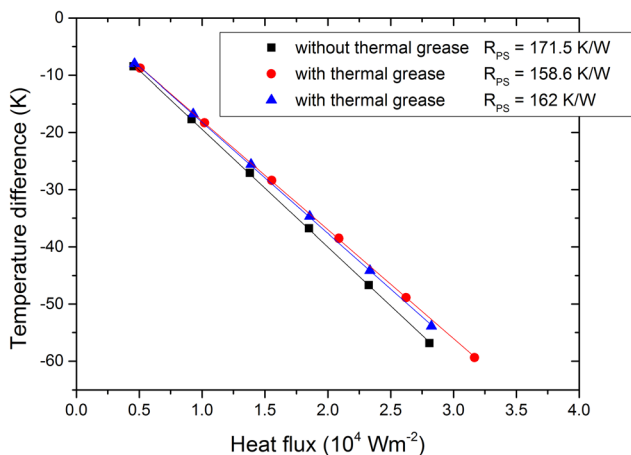


FIG. 3. Temperature difference measured at the copper blocks as a function of heat flux measured by the Peltier sensors.

known heat flux through the circuit with consequent evaluation of the temperature difference by the thermocouples. Three different examples are reported in Figure 3: two cases with thermal grease between the heat flux sensors and a third without.

Apart from the high values found for R_{PS} , which depends on the chosen heat flux sensors and can be possibly decreased by better devices, it should be noticed that the differences between them depends only on the thermal contact realized. These differences are too big with respect to the typical thermal resistance of the YIG layer of a LSSE device ($0.056\ \text{K/W}$ for the geometry of our device). As a conclusion, we better evaluate the temperature differences by the measurement of the heat flux alone through the equation $\Delta T_{\text{sample}} = -qR_{YIG}$, where R_{YIG} is the thermal resistance given by independent measurement or literature data. This approximation is valid as long as R_{YIG} is magnetic field independent. Figure 4 shows the values we obtain for the LSSE voltage, normalized with the distance of the electric contacts w_{Pt} , as a function of the heat flux for the saturating magnetic field. As expected, the normalized LSSE voltage changes sign according to the direction of heat flux and the behaviour is approximately linear. Figure 5 shows the normalized LSSE voltage as a function of the magnetic field for several heat flux values. The normalized LSSE voltage sign inversion according to the magnetization corresponds to two different polarization directions of the spin current that is generated in the YIG film, in agreement with the magnetic properties of the YIG layer. Figure 6 shows the magnetization curve of the YIG sample measured by vibrating sample magnetometer (VSM). In this figure, the LSSE electric field (normalized to the measurement heat flux) is superimposed to the magnetization curve for comparison. There is an overall agreement between the two curves which shows that the injected spin current is proportional to the magnetization of the YIG. Small differences can be understood as a consequence of the multi-domain state of the YIG at intermediate magnetization states. When we have several magnetic

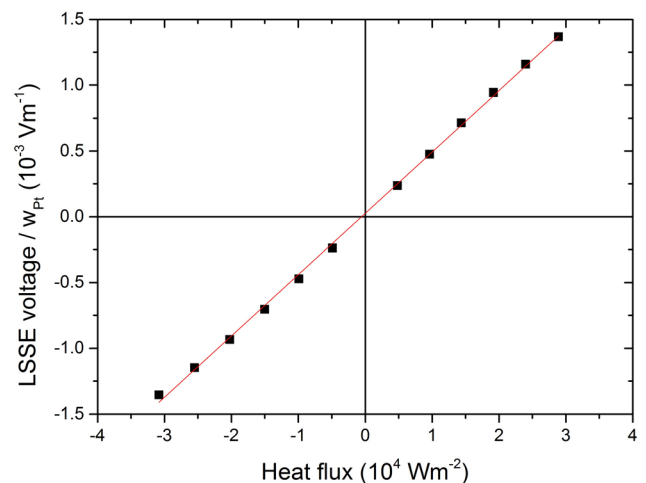


FIG. 4. LSSE voltage divided by w_{Pt} at saturation magnetic field as a function of the heat flux. This characterization of the LSSE device does not depend on the value of the thermal resistance of the interface between sample and thermal bath.

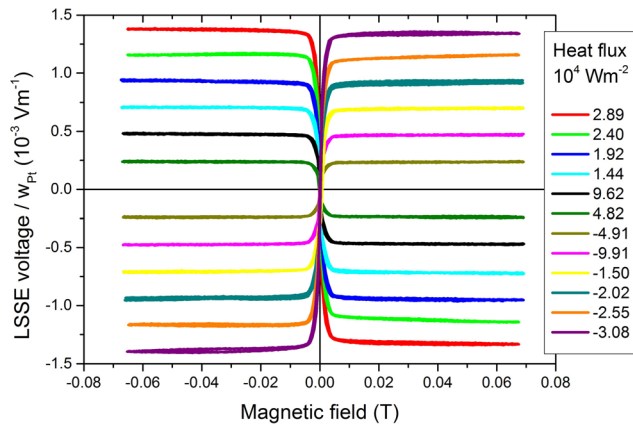


FIG. 5. Normalized LSSE voltage as a function of the external magnetic field at various heat fluxes through the sample.

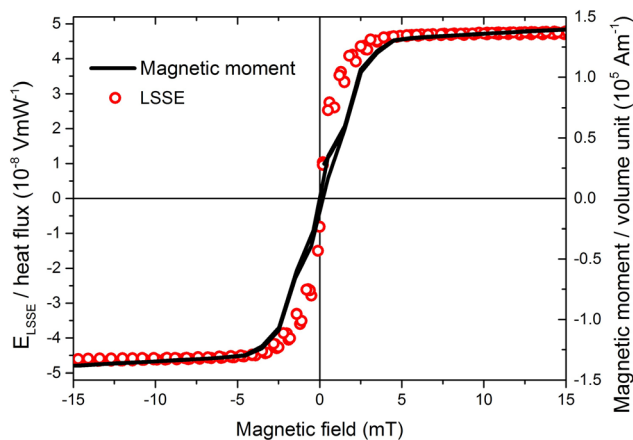


FIG. 6. Saturation magnetic field evaluated by LSSE electric field and by the vibrating sample magnetometer measurement.

domains, each of them contributes to the spin injection into the platinum and the superposition of these effects can be slightly non-linear. The result of Figure 6, in which the absolute value of the LSSE curve is above the absolute value of magnetization curve, suggests that the domains that are in majority may cause more relevant effect in terms of LSSE.

IV. CONCLUSION

A strong interest is growing around the fundamental study of LSSE and its possible applications in the field of spintronics. This facts highlight the need of standardization of the LSSE measurements techniques. For this purpose, it is necessary to develop reliable procedures for the characterization and comparison of different measurement systems and different material (i.e., garnets, ferrites, Au/YIG, Pt/YIG structures). While it is relatively well assessed how to detect the degree of spin polarization by the ISHE, it is less clear how to correctly evaluate thermal gradients in presence of necessary thermal contacts due to the measuring setup. In this work, we studied a measurement system in which the thermal circuit is characterized by the measurement of the heat flux trough a LSSE sample. When the setup is used to describe the LSSE in terms of voltage V as a function of the temperature difference ΔT , as it is usually done in literature,

the results show the predominant role of a variable: the thermal resistance between the sample and a thermal bath (see Fig. 3). This leads us to deduce that even accurate measurements, performed by different experimental setups, can be hardly comparable if the (setup dependent) measured ΔT is used as independent variable. Our study points at presenting the LSSE characteristics as a function of a more controllable (and setup independent) variable as the heat flux through the sample. This variable can be easily determined and does not depend on a crucial variable as the interface thermal resistance. In this work, we show as an example the heat flux-based characterization of a LSSE device, giving a normalized spin Seebeck voltage over the heat flux equal to $4.66 \times 10^{-8} \text{ V mW}^{-1}$. If we assume a thermal conductivity of the YIG layer¹⁶ equal to $6 \text{ W m}^{-1}\text{K}^{-1}$, the spin Seebeck coefficient for the device under investigation is about $S_{SS} = 2.8 \times 10^{-7} \text{ V/K}$, having considered the thickness of the YIG layer $t_{YIG} = 4 \mu\text{m}$ and the distance between the two contacts for the ISHE voltage measurement $w_{Pt} = 6 \text{ mm}$. The future prospective of this study includes the possibility to compare different measurement systems in order to have a set-up independent evaluation of the spin Seebeck effect from a given sample.

ACKNOWLEDGMENTS

This work has been carried out within the Joint Research Project EXL04 (SpinCal), funded by the European Metrology Research Programme. The EMRP is jointly funded by the EMRP participating countries within EURAMET and the European Union.

- ¹G. Siegel, M. C. Prestgard, S. Teng, and A. Tiwari, *Sci. Rep.* **4**, 4429 (2014).
- ²A. Kirihara, K.-i. Uchida, Y. Kajiwara, M. Ishida, Y. Nakamura, T. Manako, E. Saitoh, and S. Yorozu, *Nat. Mater.* **11**, 686–689 (2012).
- ³K. Uchida, T. Ota, H. Adachi, J. Xiao, T. Nonaka, Y. Kajiwara, G. Bauer, S. Maekawa, and E. Saitoh, *J. Appl. Phys.* **111**, 103903 (2012).
- ⁴K. Uchida, M. Ishida, T. Kikkawa, A. Kirihara, T. Murakami, and E. Saitoh, *J. Phys.: Condens. Matter* **26**, 343202 (2014).
- ⁵E. Saitoh, M. Ueda, H. Miyajima, and G. Tatara, *Appl. Phys. Lett.* **88**, 182509 (2006).
- ⁶H. Adachi, K. Uchida, E. Saitoh, J.-i. Ohe, S. Takahashi, and S. Maekawa, *Appl. Phys. Lett.* **97**, 252506 (2010).
- ⁷J. Xiao, G. E. Bauer, K. Uchida, E. Saitoh, and S. Maekawa, *Phys. Rev. B* **81**, 214418 (2010).
- ⁸C. Jaworski, J. Yang, S. Mack, D. Awschalom, J. Heremans, and R. Myers, *Nat. Mater.* **9**, 898–903 (2010).
- ⁹M. Schmid, S. Srichandan, D. Meier, T. Kuschel, J.-M. Schmalhorst, M. Vogel, G. Reiss, C. Strunk, and C. H. Back, *Phys. Rev. Lett.* **111**, 187201 (2013).
- ¹⁰D. Meier, D. Reinhardt, M. Schmid, C. H. Back, J.-M. Schmalhorst, T. Kuschel, and G. Reiss, *Phys. Rev. B* **88**, 184425 (2013).
- ¹¹S.-Y. Huang, X. Fan, D. Qu, Y. Chen, W. Wang, J. Wu, T. Chen, J. Xiao, and C. Chien, *Phys. Rev. Lett.* **109**, 107204 (2012).
- ¹²T. Kikkawa, K. Uchida, S. Daimon, Y. Shiomi, H. Adachi, Z. Qiu, D. Hou, X.-F. Jin, S. Maekawa, and E. Saitoh, *Phys. Rev. B* **88**, 214403 (2013).
- ¹³T. Kikkawa, K. Uchida, Y. Shiomi, Z. Qiu, D. Hou, D. Tian, H. Nakayama, X.-F. Jin, and E. Saitoh, *Phys. Rev. Lett.* **110**, 067207 (2013).
- ¹⁴K. Uchida, T. Kikkawa, A. Miura, J. Shiomi, and E. Saitoh, *Phys. Rev. X* **4**, 041023 (2014).
- ¹⁵H. Callen, *Thermodynamics and an Introduction to Thermostatistics* (John Wiley & Sons, New York, 1985).
- ¹⁶A. M. Hofmeister, *Phys. Chem. Miner.* **33**, 45–62 (2006).